Interactions Between Upstream Turbulent Flow and Quadrotor Thruster Dynamic Performance

Ningshan Wang*, Dom DiDominic†, Tyler Vartabedian‡, Amit K. Sanyal§, and Mark N. Glauser¶
Dept. of Mechanical Aerospace Engineering, Syracuse University, Syracuse, NY, 13244, USA

The upstream turbulent velocity field of a quadrotor unmanned aerial vehicle (UAV) and its rotor performance are investigated in experiments conducted in an outdoor wind tunnel. This research targets details on the dynamic interaction between upstream turbulent flow and UAV's attitude control performance to support the development of more robust quadrotor controllers when exposed to turbulent and gusty environments. The quadrotor is exposed to a primary stream of free-shear flow with different turbulence intensities along with varying length and time scales in order to gain interaction information. Characterization of the upstream flow field is empirically calculated based on previous research. The UAV's translational degree-of-freedom (DOF) is fixed downstream of the turbulent flow to test its rotational DOF (the attitude) controller performance within a turbulent environment. The Euler angles and their respective angular velocities are measured with the Inertial Measurement Unit (IMU) built inside the UAV flight controller.

I. Introduction

Multi-rotor unmanned aerial vehicles (UAVs) featuring new types of Vertical Take-Off and Landing (VTOL) systems have proven to be advantageous with their affordability, maintainability, and wide range of applications. There are growing concerns within the UAV industry in regards to reliability and safety [1] as UAVs feature more underdeveloped control schemes and aerodynamic properties when compared to traditional manned air systems.

The dynamic stability of a multi-rotor control scheme is critical for its safety and reliability. There have been many recent publications targeting the robustness and agility of multi-rotor control schemes [2],[3],[4],[5]. A typical multi-rotor UAV control scheme is composed of the following 4 cascaded feedback loops[4], i) the translation control ii) the attitude control iii) the attitude rate control, which generates the desired rotation speed of each rotor, iv) the brush-less-direct-current (BLDC) motor control, which is implemented on the electronic speed controller (ESC) of each BLDC motor. Most of the innovations in the previously mentioned publications focus on the two outer loops of the control scheme. The output of the third cascade (the attitude rate control loop) is usually a 4-dimensional vector, which is composed of the total desired thrust and the 3 desired axial torques. Then an approximate linear static relationship is used between the force-torque vector and the rotation-speed-square vector of the rotors [2],[3]. The relationship is shown in Eq. (1).

$$[f\ \tau_1\ \tau_2\ \tau_3]^T = K[\omega_1^2\ \omega_2^2\ \omega_3^2\ \omega_4^2]^T \tag{1}$$

Finally, the desired rotation speed of each rotor is calculated and sent to each ESC, which is the fourth cascade. It shall be noted that the linear relationship mentioned earlier is a rough approximation even when the multi-rotor is cruising through static air [6][7]. In real flight, the error of this linear model will be covered by the stability and robustness of the master controller in second and first cascade.

The UAV industry has a firm interest in designing robust control schemes under turbulent flow environments due to the majority of multi-rotor disturbances stemming from these turbulent forces. [8], [9], [6], [7]. These disturbances are concerning to the aerodynamic characteristics of a multi-rotor UAV. The blade analysis in vertical and forward flight [10] described in rotorcraft/helicopter theory is widely used in these scenarios. In [9] and [8], (1) this is still applied in the cascaded control scheme, but an artificial disturbance term is added in the master controller in the first and second cascades to cancel the nonlinear terms in the aerodynamic characteristics. In [6], [7], the ESC in the fourth cascade is

*Graduate Student, Department of Mechanical & Aerospace Engineering, Syracuse University, AIAA Student Member.
†Graduate Student, Department of Mechanical & Aerospace Engineering, Syracuse University, AIAA Student Member.
‡Graduate Student, Department of Mechanical & Aerospace Engineering, Syracuse University, AIAA Student Member.
§Associate Professor, Department of Mechanical & Aerospace Engineering, Syracuse University, AIAA Senior Member.
¶Professor, Department of Mechanical & Aerospace Engineering, Syracuse University, AIAA Fellow.

enhanced to accurately generate the desired thrust. They show satisfying performance in their experimental results. It is shown that by adding aerodynamic details properly into the slave controller design, the control performance of the entire system improves.

Multi-rotors also attract attention from the field of aerodynamics and fluid mechanics, both experimental [11],[12],[13],[14] and computational aerodynamics [15], [16],[17],[18]. Some of the publications give more details on the actuator dynamics for the propellers [11],[15],[16],[17],[18], which are concerned with the third and fourth cascades mentioned earlier. A recent study [15] uses an unusual method to show the propeller performance under turbulence in an urban area. A Computational Fluid Dynamics (CFD) tool is applied to obtain the turbulence intensity of the urban area. The turbulent term is directly added to the in-flow model of the multi-rotor propellers so that the control system performance can be tested.

In this research, the goal is to experimentally provide more details of rotor performance subjected to turbulent upstream flow. While factoring in former research on multi-rotor aerodynamics, there are hopes that these results will support more robust multi-rotor controller designs. Based on the proposed experiment in [19], a quadrotor (a common type of multi-rotor UAV) is exposed to a primary stream of turbulent free-shear flow to gain interaction information under various atmospheric conditions. Considering that the thrust of each rotor will be difficult to measure during free flight, the performance of a nonlinear attitude controller is instead tested in the incoming turbulent flow.

II. Experimental Setup

A. Outdoor Wind Tunnel

The experiment was performed in an outdoor wind tunnel at Skytop Turbulence Laboratories at Syracuse University. A mixing shear layer generator combined with a diffuser was attached to the exhaust system of the Syracuse University Anechoic Chamber to generate shear layer flow. The width of the shear layer generator at its exit is l = 1.02m. Two mixing layers were separated by a wooden plate at the exit of the device which features a honeycomb structure in the lower half to generate a flow velocity difference. The thickness of both upper and lower layers are $d = l/2$. The exit wind speed of the upper half is designed to be from U_h = 3.5m/s to U_h = 10.5m/s and the exit wind speed of the lower half is designed to be from U_l = 5m/s to U_l = 15m/s. The entire device can be seen in Fig.1. The test section for the quadrotor is placed at $x \approx$ 3m at the downstream of the shear flow generator.

Fig. 1 The Mixing Shear Flow Generator

The turbulence intensity at the test section is approximated based on the previous literature [20]. In this research, considering the shear flow generated can be treated neither as native plane jet, nor as the native plane mixing layer flow, the turbulence intensity is approximated in both ways to find the upper and lower bounds of the turbulence intensity. The turbulence intensity at the test section is expected to be $\frac{<u^2>}{U^2}$, $\frac{<v^2>}{U^2}$, $\frac{<w^2>}{U^2}$, $|\frac{<uv>}{U^2}| \approx 0.01 \sim 0.03$ [20].

B. Quadrotor UAV Setup

A medium-scale quadrotor UAV, which is shown in Fig.2, is modified to be mounted downstream of the turbulent flow. The body frame design is based on a DJI F450 platform. The propulsion system is created with T-Motor Air Gear. The maximum thrust of each rotor is 1320 g. The landing gear of the quadrotor in Fig.2 is replaced with a ball joint to fix the quadrotor's translational DOF while testing the rotational DOF (the attitude) controller. In order to attach the drone to the ball-joint, a customized mount is designed and 3D printed for the experimental setup. The picture of the quadrotor mounted in the test section is shown in Fig.3. An autopilot Pixhawk Cube system is utilized in the experiment and features the commonly used flight control software, PX4. The control performance of the PX4's nonlinear attitude controller[4] is tested in the experiment.

Fig. 2 DJI F450 Quadrotor

Fig. 3 The Modified DJI F450 Mounted Downstream of the Turbulent Flow

III. Experimental Results

The experiment is run in static air and the lower bound of the designed shear flow velocity: $U_h = 3.5$m/s and $U_l = 5$m/s. After the attitude controller is turned on, it begins to stabilize itself at the equilibrium point. The result is recorded by the log file, which is downloaded from the autopilot.

The fluctuating Euler angles from the static air experiment and turbulent flow can be seen as follows:

(a) Roll Angle in Static Air

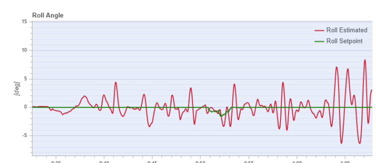

(b) Roll Angle in Turbulent Air

(c) Pitch Angle in Static Air

(d) Pitch Angle in Turbulent Air

(e) Yaw Angle in Static Air

(f) Yaw Angle in Turbulent Air

Fig. 4 Fluctuating Euler Angles in Static Air and Turbulent Upstream Flow

The fluctuating angular velocities of the Euler angles are also recorded. Note that the significant fluctuation is the measurement noise.

To test the control performance under changing desired attitude , time-varying desired attitude is set as input. It can be seen from c) and d) in 4, when desired pitch angle comes back to neural level, the pitch angle recorded in the turbulent income flow experiment shows more fluctuations.

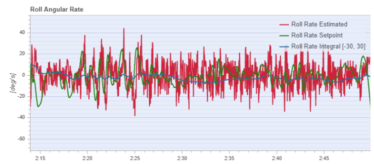

(a) Roll Angular Velocity in Static Air

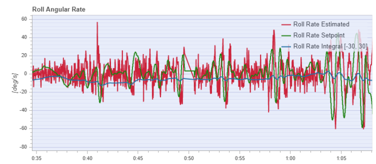

(b) Roll Angular Velocity in Turbulent Air

(c) Pitch Angular Velocity in Static Air

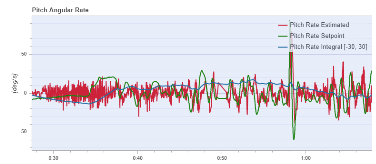

(d) Pitch Angular Velocity in Turbulent Air

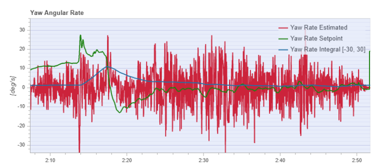

(e) Yaw Angular Velocity in Static Air

(f) Yaw Angular Velocity in Turbulent Air

Fig. 5 Angular Velocities of the Euler Angles in Static Air and Turbulent Upstream Flow

Although it is obvious that there are fluctuations in the results from both the static air experiment and the turbulent upstream flow experiment, there are no significant differences in the magnitude of the Euler angles fluctuations between the results of these two sets of data. The turbulence intensity and the average wind velocity might be overrated in the experiment with the upstream turbulence.

IV. Conclusions

The attitude controller is tested in both a static air environment and a turbulent income flow environment. The nonlinear attitude controller performance in the turbulent income flow is seen to be the same when compared with the performance in static air. The average mean velocity and turbulence intensity were too small to cause large enough fluctuations in the experiment with the turbulent upstream flow. To fix this issue, multiple experiments will be run in the future with a higher flow velocity. Multiple experiments will be run at varying speeds for comparison. On top of this, additional experiments will be run to simulate a stepfunction in the flowfield. This will be done by dropping a large rectangular board from the top of the shear flow generator. Additional experiments will also be performed in the Syracuse University subsonic wind tunnel. Here, a similar quad-rotor will be tested while utilizing a far more accurate measurement system with a variety of incoming turbulent flows.

Acknowledgements

The authors would like to thank Department of Mechanical Aerospace Engineering and the Center of Advanced Systems and Engineering (CASE) in Syracuse University and National Science Foundation award CISE 1739748 for funding and support on this research. A special thanks goes to Jean-Eric van der Elst and Alexander Dzodic for helping with a variety of aspects related to this experiment.

References

[1] Petritoli, E., Leccese, F., and Ciani, L., "Reliability and maintenance analysis of unmanned aerial vehicles," *Sensors*, Vol. 18, No. 9, 2018, p. 3171.

[2] Viswanathan, S. P., Sanyal, A. K., and Samiei, E., "Integrated guidance and feedback control of underactuated robotics system in SE (3)," *Journal of Intelligent & Robotic Systems*, Vol. 89, No. 1-2, 2018, pp. 251–263.

[3] Lee, T., Leok, M., and McClamroch, N. H., "Geometric tracking control of a quadrotor UAV on SE (3)," *49th IEEE conference on decision and control (CDC)*, IEEE, 2010, pp. 5420–5425.

[4] Brescianini, D., Hehn, M., and D'Andrea, R., "Nonlinear quadrocopter attitude control: Technical report," Tech. rep., ETH Zurich, 2013.

[5] Bangura, M., and Mahony, R., "Real-time model predictive control for quadrotors," *IFAC Proceedings Volumes*, Vol. 47, No. 3, 2014, pp. 11773–11780.

[6] Bangura, M., and Mahony, R., "Thrust control for multirotor aerial vehicles," *IEEE Transactions on Robotics*, Vol. 33, No. 2, 2017, pp. 390–405.

[7] Bangura, M., et al., "Aerodynamics and control of quadrotors," 2017.

[8] Bisheban, M., and Lee, T., "Geometric Adaptive Control for a Quadrotor UAV with Wind Disturbance Rejection," *2018 IEEE Conference on Decision and Control (CDC)*, IEEE, 2018, pp. 2816–2821.

[9] Bisheban, M., and Lee, T., "Geometric Adaptive Control with Neural Networks for a Quadrotor UAV in Wind fields," *arXiv preprint arXiv:1903.02091*, 2019.

[10] Johnson, W., *Helicopter theory*, Courier Corporation, 2012.

[11] Brandt, J., and Selig, M., "Propeller performance data at low reynolds numbers," *49th AIAA Aerospace Sciences Meeting including the New Horizons Forum and Aerospace Exposition*, 2011, p. 1255.

[12] Russell, C. R., and Sekula, M. K., "Comprehensive Analysis Modeling of Small-Scale UAS Rotors," 2017.

[13] Connors, J., Velarde, J.-M., and Glauser, M., "A Stereo-PIV Investigation of a Quadrotor Flow Field," *Bulletin of the American Physical Society*, 2018.

[14] Pandey, A., Sutkowy, M. L., McCrink, M., and Gregory, J. W., "Aerodynamic Characterization of a Quad-Rotor Helicopter," *2018 AIAA Aerospace Sciences Meeting*, 2018, p. 1526.

[15] Murray, C. W., and Anderson, D., "A CFD-based procedure for airspace integration of small unmanned aircraft within congested areas," *International Journal of Micro Air Vehicles*, Vol. 9, No. 4, 2017, pp. 235–252.

[16] Yoon, S., Lee, H. C., and Pulliam, T. H., "Computational Analysis of Multi-Rotor Flows," *54th AIAA Aerospace Sciences Meeting*, 2016, p. 0812.

[17] Ventura Diaz, P., and Yoon, S., "High-fidelity computational aerodynamics of multi-rotor unmanned aerial vehicles," *2018 AIAA Aerospace Sciences Meeting*, 2018, p. 1266.

[18] Thibault, S., Holman, D., Garcia, S., and Trapani, G., "CFD Simulation of a Quad-Rotor UAV with Rotors in Motion Explicitly Modeled Using an LBM Approach with Adaptive Refinement," *55th AIAA Aerospace Sciences Meeting*, 2017, p. 0583.

[19] Wang, N., Connors, J., Velarde, J.-M., and Glauser, M., "Interactions between upstream turbulent flow and quadrotor thruster controller performance," *Bulletin of the American Physical Society*, 2018.

[20] Pope, S. B., "Turbulent flows," , 2001.